

Stabilization of Energy-Conserving Gaits for Point-Foot Planar Biped

Aakash Khandelwal, Nilay Kant, and Ranjan Mukherjee

Abstract—The problem of designing and stabilizing impact-free, energy-conserving gaits is considered for underactuated, point-foot planar bipeds. Virtual holonomic constraints are used to design energy-conserving gaits. A desired gait corresponds to a periodic hybrid orbit and is stabilized using the Impulse Controlled Poincaré Map approach. Numerical simulations for the case of a five-link biped demonstrate convergence to a desired gait from arbitrary initial conditions.

I. INTRODUCTION

Point-foot bipeds represent a class of underactuated systems whose dynamics are hybrid due to foot-ground interaction and interchange of stance and swing legs. An important control problem is to design and stabilize a biped gait, which is a periodic hybrid orbit. Virtual Holonomic Constraints (VHCs) [1]–[3] have been used to design gaits for bipeds; systematic selection of VHCs and parameter optimization have been used to guarantee stability of gaits [1], [4]–[9].

In this work, we consider point-foot planar bipeds having n degrees-of-freedom (DOFs) and $(n-1)$ control inputs. For this class of systems, we design and stabilize *energy-conserving* gaits, that conserve mechanical energy of the biped over each step and are free from impact during foot-ground interaction. The notion of an energy-conserving gait appeared in [10]; here it is formally described using VHCs, and designed to satisfy conditions for feasibility and stabilizability. Such gaits can be expressed as hybrid orbits that are invariant to coordinate relabelling. The Impulse Controlled Poincaré Map (ICPM) approach, which has been used to stabilize both continuous and hybrid orbits [11], [12], is used for stabilizing a desired energy-conserving gait from arbitrary initial conditions. The efficacy of the control design is demonstrated through a case study of the five-link biped.

II. SYSTEM DYNAMICS

A. System Description and Assumptions

Consider the n -link planar biped (n is odd) comprised of a single-link torso and kinematically similar legs with point feet - see Fig.1. It is assumed that the biped gait is comprised of a sequence of steps, where each step is comprised of a single-support phase (one leg is in contact with the ground) and a double-support phase (both legs are in contact with the ground). In the single-support phase, the leg in contact with the ground is referred to as the stance leg and the other leg is referred to as the swing leg. The stance foot is passive; it does not slide or leave the ground and acts as a frictionless pivot. The single-support phase ends when the swing leg comes in contact with the ground. The ensuing double-support phase

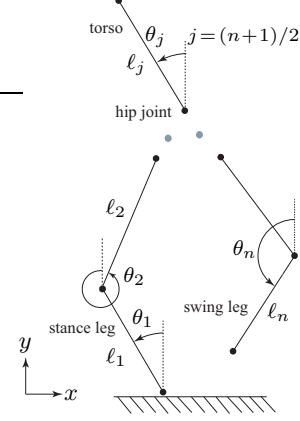


Fig. 1. An n -link point-foot planar biped.

is of infinitesimal time duration; during this phase, there is physical interaction between the ground and the swing leg but not between the ground and the stance leg. The double-support phase ends with relabelling of coordinates for interchange of the stance and swing legs.

Each leg has $(n-1)/2$ links; the stance leg links are numbered sequentially 1 through $(n-1)/2$ starting from the link in contact with the ground, the torso is link $(n+1)/2$, and the swing leg links are numbered sequentially $(n+3)/2$ through n starting from the link in contact with the torso. The length of the j -th link, $j = 1, 2, \dots, n$, is l_j . Since the legs are kinematically identical, the link lengths satisfy

$$l_{n-j+1} = l_j \quad \forall j = 1, 2, \dots, (n-1)/2$$

The orientation of the j -th link, $j = 1, 2, \dots, n$, measured counter-clockwise with respect to the vertical, is denoted by θ_j , $\theta_j \in S^1$. The link j , $j = 2, \dots, n$, is driven by an actuator mounted on link $(j-1)$, which applies torque τ_j .

The dynamics of the biped gait in the single-support phase, also known as the swing phase, is discussed in section II-B. The dynamics of foot-ground interaction and the relabelling of coordinates for interchange of the stance and swing legs in the double-support phase is discussed in section II-C. For generality and ease of control design, the dynamics are presented using the generalized coordinates $q \in \mathcal{Q}^n \triangleq \prod_{j=1}^n S^1$, $q \triangleq [q_1^T \quad q_2]^T$, where $q_1 \in \mathcal{Q}^{n-1}$ and $q_2 \in S^1$. We define the generalized coordinates q as follows

$$q_1 = [(\theta_2 - \theta_1) \quad (\theta_3 - \theta_2) \quad \dots \quad (\theta_n - \theta_{n-1})], \quad q_2 = \theta_1$$

B. Swing Phase Dynamics

During the swing phase, the biped represents an n -DOF underactuated system with one passive DOF q_2 . The kinetic and potential energies of the system are denoted by $T(q, \dot{q}) =$

$\frac{1}{2}\dot{q}^T M(q)\dot{q}$ and $V(q)$ respectively, where $M \in R^{n \times n}$ is the symmetric, positive definite mass matrix:

$$M(q) = \begin{bmatrix} M_{11}(q) & M_{12}(q) \\ M_{12}^T(q) & M_{22}(q) \end{bmatrix}$$

where $M_{11} \in R^{(n-1) \times (n-1)}$, $M_{22} \in R$ and the equations of motion can be written in the same form as in [11]:

$$M_{11}(q)\ddot{q}_1 + M_{12}(q)\ddot{q}_2 + h_1(q, \dot{q}) = u \quad (1a)$$

$$M_{12}^T(q)\ddot{q}_1 + M_{22}(q)\ddot{q}_2 + h_2(q, \dot{q}) = 0 \quad (1b)$$

where $[h_1^T \ h_2^T]^T \in R^n$ is the vector of Coriolis, centrifugal, and gravity forces, and $u = [\tau_2 \ \tau_3 \ \dots \ \tau_n]^T \in R^{n-1}$ is the vector of control inputs. Since the biped has revolute joints, we make the following assumption [3], [11].

Assumption 1: For the n -link biped, the mass matrix and the potential energy are even functions of q :

$$M(q) = M(-q), \quad V(q) = V(-q)$$

which satisfies [11, Assumption 1].

When u is continuous and has the form $u = u_c(q, \dot{q})$, the dynamics in (1) has the state-space representation

$$\dot{x} = f(x), \quad x \triangleq [q^T \ \dot{q}^T]^T \in \mathcal{Q}^n \times R^n \quad (2)$$

If an impulsive input $u_{\mathcal{I}}$ is applied in addition to u_c at any instant, the system will experience a discontinuous change in the generalized velocities with no change in the generalized coordinates [11], [13]. The jump in generalized velocities can be obtained by integrating (1) as follows:

$$\begin{bmatrix} M_{11} & M_{12} \\ M_{12}^T & M_{22} \end{bmatrix} \begin{bmatrix} \Delta \dot{q}_1 \\ \Delta \dot{q}_2 \end{bmatrix} = \begin{bmatrix} \mathcal{I} \\ 0 \end{bmatrix}, \quad \mathcal{I} \triangleq \int_0^{\Delta t} u_{\mathcal{I}} dt \quad (3)$$

where Δt is the infinitesimal duration for which $u_{\mathcal{I}}$ is active, $\mathcal{I} \in R^{n-1}$ is the impulse of $u_{\mathcal{I}}$,

$$\Delta \dot{q}_1 \triangleq (\dot{q}_1^+ - \dot{q}_1^-), \quad \Delta \dot{q}_2 \triangleq (\dot{q}_2^+ - \dot{q}_2^-)$$

and $(\cdot)^-$ and $(\cdot)^+$ denote the variable (\cdot) immediately before and after an event where there is a discontinuous jump in its value. The states immediately after application of the impulsive input can be expressed as

$$x^+ = x^- + \Delta x_{\mathcal{I}}, \quad \Delta x_{\mathcal{I}} \triangleq \begin{bmatrix} 0 \\ \Delta \dot{q} \end{bmatrix} \quad (4)$$

where $\Delta \dot{q}$ is obtained from (3).

C. Foot-Ground Interaction and Coordinate Relabelling

In the double-support phase, there is impulsive interaction between the swing foot and the ground. Simultaneously, the stance foot lifts from the ground without interaction, and there is an instantaneous interchange between stance and swing legs.

Following the approach in [1], [14], the impact between the swing foot and the ground is modeled as an inelastic collision. This model is described using $(n+2)$ DOF, that include the original n DOFs and the two Cartesian coordinates of the stance foot (s_x, s_y) , $s_x, s_y \in R$. The

equations of motion of the extended system can be written in the form

$$M_e(q_e)\ddot{q}_e + h_e(q_e, \dot{q}_e) = p_e + p^{\text{ext}}, \quad q_e \triangleq [q^T \ s_x \ s_y]^T \quad (5)$$

where $M_e \in R^{(n+2) \times (n+2)}$ is the mass matrix, $h_e \in R^{n+2}$ is the vector of Coriolis, centrifugal, and gravity forces, $p_e = [u^T \ 0 \ 0 \ 0]^T \in R^{n+2}$ is the vector of generalized forces, and $p^{\text{ext}} \in R^{n+2}$ is the vector of generalized impulsive forces due to interaction between the swing foot and the ground. The discontinuous change in the generalized velocities due to p^{ext} can be obtained by integrating (5)

$$M_e(q_e) \Delta \dot{q}_e = \mathcal{I}^{\text{ext}}, \quad \mathcal{I}^{\text{ext}} \triangleq \int_0^{\Delta t} p^{\text{ext}} dt \quad (6)$$

where Δt is the infinitesimal duration of the impact, $\mathcal{I}^{\text{ext}} \in R^{n+2}$ is the impulse due to p^{ext} , and $\Delta \dot{q}_e \triangleq (\dot{q}_e^+ - \dot{q}_e^-)$. Let F_x and F_y denote the Cartesian components of the impulsive forces on the swing foot due to impact. Then

$$p^{\text{ext}} = \Gamma^T F, \quad \Gamma \triangleq \frac{\partial \gamma}{\partial q_e}, \quad \gamma \triangleq \begin{bmatrix} \gamma_x \\ \gamma_y \end{bmatrix}, \quad F \triangleq \begin{bmatrix} F_x \\ F_y \end{bmatrix} \quad (7)$$

where $\gamma \equiv \gamma(q_e) \in R^2$ denotes the Cartesian coordinates of the swing foot. By integrating (7) over the duration of impact Δt , we get

$$\mathcal{I}^{\text{ext}} = \Gamma^T \mathcal{I}_g, \quad \mathcal{I}_g \triangleq \int_0^{\Delta t} F dt \quad (8)$$

Since the foot-ground collision is inelastic,

$$\Gamma \dot{q}_e^+ = 0 \quad (9)$$

Using (6), (8) and (9), we get

$$\begin{bmatrix} M_e & -\Gamma^T \\ \Gamma & 0 \end{bmatrix} \begin{bmatrix} \dot{q}_e^+ \\ \mathcal{I}_g \end{bmatrix} = \begin{bmatrix} M_e \dot{q}_e^- \\ 0 \end{bmatrix} \quad (10)$$

The states immediately after foot-ground interaction are

$$x^+ = x^- + \Delta x_g, \quad \Delta x_g \triangleq \begin{bmatrix} 0 \\ \Delta \dot{q} \end{bmatrix} \quad (11)$$

where $\Delta \dot{q}$ is obtained using (10).

The subsequent interchange of the stance and swing legs is equivalent to a relabelling of states [7]. The states immediately after leg interchange are a function of those immediately before interchange, and is given by the relation:

$$x^+ = \mathcal{R}(x^-) \quad (12)$$

$$\mathcal{R}(x) = \text{blockdiag} [V \ V] x + [\Pi^T \ | \ 0_{1 \times n}]^T$$

where $V \in R^{n \times n}$ and $\Pi \in R^n$ have elements given by

$$V_{ij} = \begin{cases} -1 & i+j = n \\ 1 & i = n \\ 0 & \text{otherwise} \end{cases} \quad \Pi_i = \begin{cases} \pi & i = (n-1)/2 \\ -\pi & i = \{(n+1)/2, n\} \\ 0 & \text{otherwise} \end{cases}$$

where $0_{i \times j} \in R^{i \times j}$ is the matrix of zeros.

D. Hybrid Dynamic Model

The hybrid dynamics of the gait is described as follows:

$$\mathcal{D} : \begin{cases} \dot{x} = f(x), & x \notin \mathcal{S}, u_{\mathcal{I}} = 0 & \textcircled{1} \\ x^+ = x^- + \Delta x_{\mathcal{I}}, & x^- \notin \mathcal{S}, u_{\mathcal{I}} \neq 0 & \textcircled{2} \\ x^+ = x^- + \Delta x_g, & x^- \in \mathcal{S}_1 & \textcircled{3} \\ x^+ = \mathcal{R}(x^-), & x^- \in \mathcal{S}_2 & \textcircled{4} \end{cases} \quad (13)$$

where

$$\mathcal{S}_1 \triangleq \{x \in \mathcal{Q}^n \times \mathcal{R}^n : \gamma_y = 0, \dot{\gamma}_y < 0\} \quad (14a)$$

$$\mathcal{S}_2 \triangleq \{x \in \mathcal{Q}^n \times \mathcal{R}^n : \gamma_y = 0, \dot{\gamma}_y = 0\} \quad (14b)$$

and $\mathcal{S} \triangleq \mathcal{S}_1 \cup \mathcal{S}_2$ is the set of states during the double-support phase. The different components of the hybrid dynamics \mathcal{D} over a step are illustrated with the help of Fig.2 for a single impulsive actuation during the swing phase.

III. ENERGY-CONSERVING GAITS

We define an energy-conserving gait as one where the biped has equal mechanical energy at the beginning and end of the swing phase, and there is no loss of energy when the swing leg comes in contact with the ground. The conditions for a gait to be energy conserving are expressed in terms of θ_j and $\dot{\theta}_j$, $j = 1, 2, \dots, n$, to aid physical understanding. Let $(\cdot)^i$ and $(\cdot)^f$ denote the value of (\cdot) at the beginning and end of the swing phase.

A. Sufficient Conditions for an Energy-Conserving Gait

A gait will be energy-conserving if the following conditions are satisfied:

- The potential energy at the beginning and end of the swing phase are identical, *i.e.*

$$\theta_j^f = -\theta_j^i, \quad j = 1, 2, \dots, n \quad (15)$$

- The kinetic energy at the beginning and end of the swing phase are identical, *i.e.*

$$\dot{\theta}_j^f = \dot{\theta}_j^i, \quad j = 1, 2, \dots, n \quad (16)$$

- The interaction between the swing leg and the ground at the end of the swing phase is impact-free, *i.e.*

$$\dot{\gamma}^f = - \sum_{\substack{j=1 \\ j \neq (n+1)/2}}^n \ell_j \begin{bmatrix} \cos \theta_j^f \\ \sin \theta_j^f \end{bmatrix} \dot{\theta}_j^f = 0 \quad (17)$$

where link $(n+1)/2$ is the torso and hence excluded.

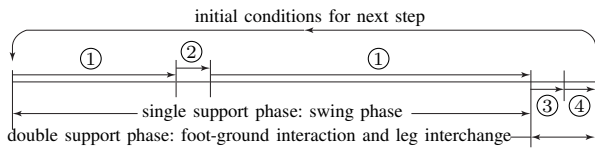


Fig. 2. Hybrid dynamics of biped over a step with a single impulsive actuation during the swing phase. The different components are:

- ①: continuous-time dynamics,
- ②: jump in states due to impulsive actuation,
- ③: jump in states due to foot-ground in interaction, and
- ④: change of states due to coordinate relabelling.

B. Gait Design Using VHCs

To satisfy (15), we first make the assumption:

Assumption 2: The orientation of the passive link, link 1, is symmetric with respect to the vertical at the beginning and the end of the swing phase, *i.e.*, $\theta_1^f = -\theta_1^i$.

Next, we impose the following VHCs [3], [11] on the actuated joint trajectories during swing phase

$$\theta_j = a_j \theta_1 + k_j \pi + f_j^o(\theta_1), \quad j = 2, 3, \dots, n \quad (18)$$

where $a_j \in \mathcal{R}$ and $k_j \in \mathcal{Z}$ are constants, and $f_j^o(\theta_1)$ is an odd function. The VHCs, along with Assumption 2, ensure that (15) is satisfied for all actuated joint angles. This is true because $k_j \pi = -k_j \pi \forall k_j \in \mathcal{Z}$ and $\theta_j \in \mathcal{S}^1$.

Taking the time derivative of (18), we obtain

$$\dot{\theta}_j = \left[a_j + \frac{df_j^o}{d\theta_1} \right] \dot{\theta}_1, \quad j = 2, 3, \dots, n \quad (19)$$

In the above equation, $[a_j + (df_j^o/d\theta_1)]$ is an even function of θ_1 ; therefore (16) will be satisfied if $\dot{\theta}_1$ is an even function of θ_1 . We will show in section III-D that this requirement can be satisfied for the choice of VHCs in (18). The condition in (17) can be satisfied by choosing the VHC parameters judiciously.

C. Constraints on VHC Parameters

For a single-step periodic gait, we impose the condition that the biped has the same configuration at the beginning of the swing phase. This implies that the biped configuration at the beginning and end of the swing phase is symmetric about the vertical passing through the stance foot, *i.e.*,

$$\theta_{n-j+1}^f = \theta_j^i - \pi \quad \forall j = 1, 2, \dots, (n-1)/2 \quad (20a)$$

$$\theta_j^f = \theta_j^i \quad j = (n+1)/2 \quad (20b)$$

Using (15), we get

$$\theta_{n-j+1}^i = -\theta_j^i + \pi \quad \forall j = 1, 2, \dots, (n-1)/2 \quad (21a)$$

$$\theta_j^i = -\theta_j^i \quad j = (n+1)/2 \quad (21b)$$

From (21b), it follows

$$\theta_j^i = 0 \quad j = (n+1)/2 \quad (22)$$

The joint velocities must satisfy

$$\dot{\theta}_{n-j+1}^f = \dot{\theta}_j^i \quad \forall j = 1, 2, \dots, (n-1)/2 \quad (23)$$

Using (16), we get

$$\dot{\theta}_{n-j+1}^i = \dot{\theta}_j^i \quad \forall j = 1, 2, \dots, (n-1)/2 \quad (24)$$

By substituting (15) and (16) in (17), we obtain

$$\sum_{\substack{j=1 \\ j \neq (n+1)/2}}^n \ell_j \begin{bmatrix} \cos \theta_j^i \\ -\sin \theta_j^i \end{bmatrix} \dot{\theta}_j^i = 0 \quad (25)$$

Since the legs are kinematically identical, substitution of (21) and (24) into (25) yields

$$\sum_{j=1}^{(n-1)/2} \ell_j \sin \theta_j^i \dot{\theta}_j^i = 0 \quad (26)$$

It should be noted that the first equation in (25) is trivially satisfied.

Remark 1: It follows from (19) that the constraints in (24) and (26) are independent of the value of θ_1^i . Thus, the $n+1$ constraints in (21a), (22), (24) and (26) depend only on the choice of θ_1^i .

D. Zero Dynamics of Energy-Conserving Gait

In terms of the generalized coordinates, the VHCs in (18), with parameters chosen subject to the constraints in (21a), (22), (24) and (26), are expressed as follows:

$$\rho(q) = q_1 - \Phi(q_2) = 0, \quad \Phi : S^1 \rightarrow \mathcal{Q}^{n-1} \quad (27)$$

The corresponding constraint manifold \mathcal{C} is given by:

$$\mathcal{C} = \left\{ (q, \dot{q}) : q_1 = \Phi(q_2), \dot{q}_1 = \left[\frac{\partial \Phi}{\partial q_2} \right] \dot{q}_2 \right\} \quad (28)$$

Remark 2: Since the generalized coordinates are linear combinations of θ_j 's, and linear combinations of odd functions are odd, the function $\Phi(q_2)$ is odd in q_2 , i.e., $\Phi(q_2) = \Phi(-q_2)$, which satisfies [11, Assumption 2].

Remark 3: The VHCs are chosen such that $M_{12}^T(\partial\Phi/\partial q_2) + M_{22} \neq 0$; this ensures that the VHC in (27) is regular and \mathcal{C} is stabilizable [11, Remark 2].

For initial conditions on \mathcal{C} , the continuous control u_c in [11] enforces the VHC and renders \mathcal{C} controlled invariant. On \mathcal{C} , the system satisfies $q_1 \equiv \Phi(q_2)$. By substituting (27) in (1b), we get the swing phase zero dynamics [11], [15]:

$$\ddot{q}_2 = \alpha_1(q_2) + \alpha_2(q_2)\dot{q}_2^2 \quad (29)$$

It can be shown that \ddot{q}_2 is an odd function of q_2 since the VHCs in (27) are odd. This implies that both α_1 and α_2 are odd functions of q_2 ; and \dot{q}_2 is either an even function or an odd function of q_2 , but not neither. The zero dynamics in (29) has an integral of motion $E(q_2, \dot{q}_2)$ [2], [3], and its qualitative properties can be described by a potential energy function $\mathcal{P}(q_2)$, which has minimum and maximum values \mathcal{P}_{\min} and \mathcal{P}_{\max} [3]. For an energy level set $E(q_2, \dot{q}_2) = c$, $c \in (\mathcal{P}_{\min}, \mathcal{P}_{\max})$ corresponds to a periodic orbit where \dot{q}_2 changes sign periodically (\dot{q}_2 is an odd function of q_2) and $c > \mathcal{P}_{\max}$ corresponds to an orbit where \dot{q}_2 does not change sign (\dot{q}_2 is an even function of q_2) [3], [11]. If \dot{q}_2 changes sign when q_2 changes sign, the biped will not be able to complete a step. Therefore, a feasible biped gait is a periodic orbit where \dot{q}_2 does not change sign. This will be accomplished through proper choice of initial conditions that result in $c > \mathcal{P}_{\max}$.

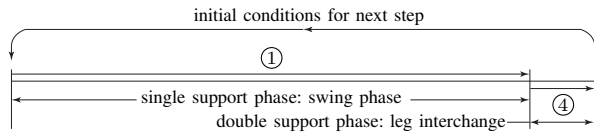


Fig. 3. Hybrid dynamics of biped over a step for an energy-conserving gait; it is a simpler version of the dynamics shown in Fig.2. The different components are:

- ①: continuous-time dynamics,
- ④: change of states due to coordinate relabelling.

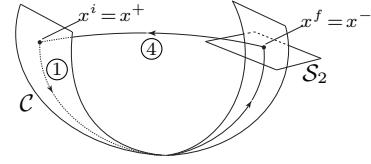


Fig. 4. Evolution of system trajectory during an energy-conserving gait.

A system trajectory in \mathcal{C} satisfies $\dot{\gamma}^f = 0 \forall x \in \mathcal{C}$. Thus, $\mathcal{C} \cap \mathcal{S}_1 = \emptyset$ and consequently $\mathcal{C} \cap \mathcal{S} = \mathcal{C} \cap \mathcal{S}_2$. A trajectory evolving in \mathcal{C} in the single-support phase will intersect \mathcal{S}_2 in the double-support phase. This results in a discontinuous jump in states described by (12). Although the trajectory may leave \mathcal{C} during the jump, it can be shown that the new states lie in \mathcal{C} , i.e., \mathcal{C} is invariant under relabelling of the states:

$$\mathcal{R}(\mathcal{C} \cap \mathcal{S}_2) \subset \mathcal{C} \quad (30)$$

The components of the hybrid dynamics over a step for an energy-conserving gait are shown in Fig.3; the evolution of the system trajectory is shown in Fig.4.

IV. STABILIZATION OF AN ENERGY-CONSERVING GAIT

A. Orbit Describing an Energy-Conserving Gait

An energy-conserving gait, defined by the VHCs in (27), is described by the hybrid orbit:

$$\mathcal{O}^* = \mathcal{O}_c^* \cup \mathcal{O}_R^* \quad (31)$$

where

$$\begin{aligned} \mathcal{O}_c^* &= \{x \in \mathcal{C} : E(q_2, \dot{q}_2) = c^*\} \quad c^* > \mathcal{P}_{\max} \quad (32a) \\ \mathcal{O}_R^* &= \{x^-, x^+ : x^- \in \mathcal{O}_c^* \cap \mathcal{S}_2, x^+ = \mathcal{R}(x^-) \in \mathcal{O}_c^*\} \quad (32b) \end{aligned}$$

The orbit \mathcal{O}^* is stabilized using the ICPM approach [11], whose efficacy has been demonstrated for both continuous and hybrid orbits [11], [12].

B. Poincaré Map

To stabilize the orbit \mathcal{O}^* from any point in its neighborhood, we describe the hybrid dynamics in (13) using a discrete-time map. To this end, we define the Poincaré section:

$$\Sigma = \{x \in \mathcal{Q}^n \times \mathcal{R}^n : q_2 = q_2^*, \dot{q}_2 < 0\} \quad (33)$$

The states on Σ are:

$$z = [q_1^T \quad \dot{q}^T]^T, \quad z \in \mathcal{Q}^{n-1} \times \mathcal{R}^n \quad (34)$$

We assume that impulsive actuation is applied when the system trajectory intersects Σ . If $z(k)$ denotes the states immediately prior to application of \mathcal{I} , the hybrid dynamics of the impulse-controlled system can be expressed as

$$z(k+1) = \mathbb{P}[z(k), \mathcal{I}(k)] \quad (35)$$

The map \mathbb{P} captures the dynamics between subsequent intersections of the system trajectory with Σ . It is comprised of the components ②, ①, ③, ④, and ①, described in (13) and depicted in Fig.2.

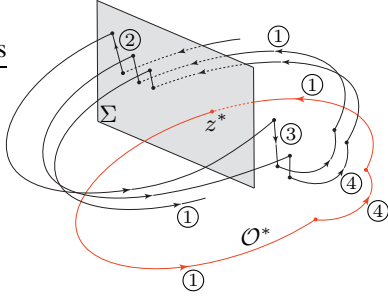


Fig. 5. Schematic of the ICPM approach to orbital stabilization of an energy-conserving gait. The desired orbit is shown in red. The different components of the hybrid dynamics, namely, ①, ②, ③ and ④ are described by (13).

C. Orbital Stabilization

If $x \in \mathcal{O}^*$, the system trajectory is restricted to \mathcal{O}^* under continuous control u_c . The intersection of \mathcal{O}^* with Σ is therefore a fixed point $z(k) = z^*$, $\mathcal{I}(k) = 0$ of \mathbb{P}

$$z^* = \mathbb{P}(z^*, 0) \quad (36)$$

If $x \notin \mathcal{O}^*$, u_c does not guarantee convergence of the trajectory to \mathcal{O}^* , and the impulsive inputs $\mathcal{I}(k)$ are used to asymptotically stabilize the fixed point z^* , and consequently the orbit \mathcal{O}^* [11], [16]. To this end, we linearize the map \mathbb{P} about $z(k) = z^*$ and $\mathcal{I}(k) = 0$ as follows:

$$e(k+1) = \mathcal{A}e(k) + \mathcal{B}\mathcal{I}(k), \quad e(k) \triangleq z(k) - z^* \quad (37)$$

where

$$\begin{aligned} \mathcal{A} &\triangleq [\nabla_z \mathbb{P}(z, \mathcal{I})]_{z=z^*, \mathcal{I}=0} \\ \mathcal{B} &\triangleq [\nabla_{\mathcal{I}} \mathbb{P}(z, \mathcal{I})]_{z=z^*, \mathcal{I}=0} \end{aligned} \quad (38)$$

The matrices $\mathcal{A} \in R^{(2n-1) \times (2n-1)}$ and $\mathcal{B} \in R^{(2n-1) \times (n-1)}$ can be computed numerically. If $(\mathcal{A}, \mathcal{B})$ is controllable, the orbit \mathcal{O}^* can be stabilized by the discrete feedback:

$$\mathcal{I}(k) = \mathcal{K}e(k) \quad (39)$$

where \mathcal{K} is chosen such that the eigenvalues of $(\mathcal{A} + \mathcal{B}\mathcal{K})$ lie inside the unit circle.

The stabilization of \mathcal{O}^* using the ICPM approach [11], [12] is explained with the help of Fig.5. The desired orbit \mathcal{O}^* (shown in red), intersects Σ at the fixed point z^* ; it corresponds to an energy-conserving gait where the states undergo a single discontinuous jump due to coordinate relabelling - see Fig.4. For a trajectory not on \mathcal{O}^* (shown in black), there is a discontinuous jump in states on Σ due to application of $\mathcal{I}(k)$. A second discontinuous jump occurs at the time of foot-ground interaction; this is immediately followed by the discontinuous jump due to coordinate relabelling. The input $\mathcal{I}(k)$ in (39) guarantees asymptotic convergence of a system trajectory to \mathcal{O}^* .

V. GAIT STABILIZATION FOR FIVE-LINK BIPED

A. Gait Selection

For $n = 5$, (26) has the form

$$\ell_1 \sin \theta_1^i \dot{\theta}_1^i + \ell_2 \sin \theta_2^i \dot{\theta}_2^i = 0 \quad (40)$$

TABLE I

KINEMATIC AND DYNAMIC PARAMETERS OF FIVE-LINK BIPED

j	ℓ_j (m)	d_j (m)	m_j (kg)	J_j (kg m ²)
1, 5	0.5000	0.2500	0.4000	0.0083
2, 4	0.5500	0.2750	0.4500	0.0113
3 (torso)	0.6000	0.3000	0.5500	0.0165

TABLE II

VHC PARAMETERS FOR ENERGY-CONSERVING GAIT

j	a_j	k_j	\mathcal{G}_j	\mathcal{H}_j
2	0.5500	0	0.2717	8
3 (torso)	0.0000	0	-0.4000	8
4	-0.5500	1	0.1342	8
5	-1.6833	1	-0.3795	10

which permits us to obtain a non-trivial gait. We seek a gait where the odd functions $f_j^o(\theta_1)$ in (18) are sinusoidal. Thus (18) can be rewritten as:

$$\theta_j = a_j \theta_1 + k_j \pi + \mathcal{G}_j \sin(\mathcal{H}_j \theta_1), \quad j = 2, 3, 4, 5 \quad (41)$$

where $\mathcal{G}_j, \mathcal{H}_j \in R$, $j = 2, 3, 4, 5$, are constants. For a certain choice of θ_1^i , the 16 VHC parameters in (41) should satisfy the six constraints in (21a), (22), (24) and (40). For the kinematic and dynamic parameters in Table I, and the choice $\theta_1^i = \pi/8$, a set of feasible VHC parameters which ensure a realistic walking motion are listed in Table II.

Using (41) and the parameters in Table II, (27) can be expressed as:

$$\begin{aligned} \rho(q) &= q_1 - \Phi(q_2) = 0, \quad \Phi : S^1 \rightarrow Q^4 \\ \Phi(q_2) &= \begin{bmatrix} -0.4500q_2 + 0.2717 \sin(8q_2) \\ -0.5500q_2 - 0.6717 \sin(8q_2) \\ -0.5500q_2 + \pi + 0.5342 \sin(8q_2) \\ -1.1333q_2 - 0.1342 \sin(8q_2) - 0.3795 \sin(10q_2) \end{bmatrix} \end{aligned} \quad (42)$$

The above VHC satisfies the conditions in remarks 2 and 3, and is enforced by the continuous control u_c in [11]¹. The desired orbit \mathcal{O}^* , defined by (31) and (32) is chosen to be the one which passes through $(q_2, \dot{q}_2) = (\pi/8, -5\pi/3)$, for which the sign of \dot{q}_2 does not change.

Remark 4: There is significant flexibility in the choice of VHCs and their parameters.

B. Stabilization of \mathcal{O}^*

We choose the following Poincaré section:

$$\Sigma = \{x \in Q^5 \times R^5 : q_2 = \pi/16, \dot{q}_2 < 0\} \quad (43)$$

on which the states are denoted by $z, z \in Q^4 \times R^5$, defined in (34). The intersection of \mathcal{O}^* with Σ in (43) is the fixed point z^* of the map \mathbb{P} , and satisfies (36). The matrices $\mathcal{A} \in R^{9 \times 9}$ and $\mathcal{B} \in R^{9 \times 4}$ in (38) are computed numerically [11]; their expressions are not provided here for brevity. It is seen that the eigenvalues of \mathcal{A} do not all lie within the unit circle, but the pair $(\mathcal{A}, \mathcal{B})$ is controllable. The gain matrix \mathcal{K} in (39),

¹The expression for u_c uses the gains $k_p = 750I_4$ and $k_d = 25I_4$, where $I_n \in R^{n \times n}$ is the identity matrix; these gains were chosen to ensure rapid convergence of the trajectories to the constraint manifold \mathcal{C} .

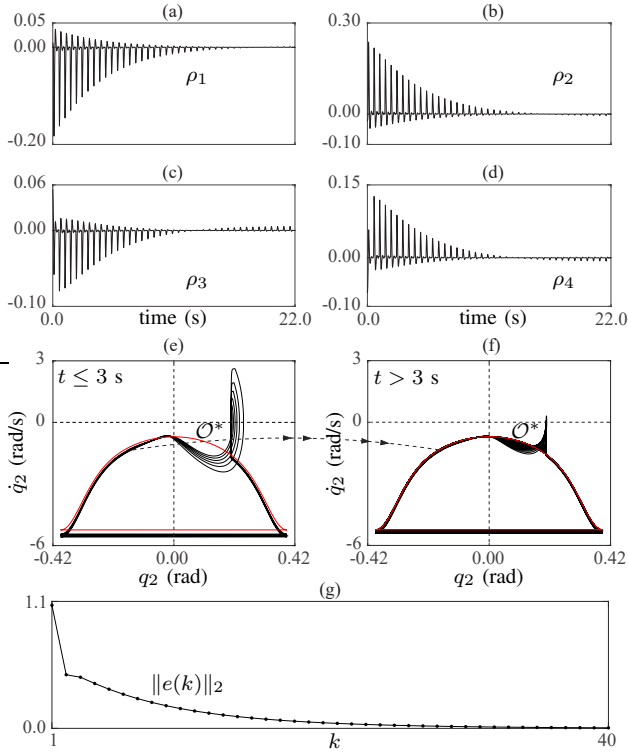


Fig. 6. Orbital stabilization of an energy-conserving gait using the ICPM approach: (a)-(d) show the components of $\rho(q)$, (e) and (f) show the phase portrait of the passive coordinate, and (g) shows the norm of the error in states on the Poincaré section.

which asymptotically stabilizes \mathcal{O}^* , is obtained using LQR; the gain matrices were chosen as

$$Q = \text{blockdiag} [I_4 \quad 1.5I_5], \quad R = I_4$$

C. Simulation results

For an arbitrary set of initial conditions not lying on \mathcal{O}^* , simulation results of the ICPM approach to gait stabilization are shown in Fig.6 for 40 steps, that corresponds to a duration of approx. 22 s. For the biped walking with the desired energy-conserving gait, a single step is completed in 0.5646 s under the continuous control u_c . The impulsive control in (39) is realized in the simulations using high-gain feedback u_{hg} , as in [11]²; the components of $\rho(q)$ are plotted in Fig.6(a)-(d); these plots demonstrate convergence of system trajectories to the constraint manifold \mathcal{C} . The phase portrait of the passive coordinate q_2 is shown in Fig.6(e) for $t \leq 3$ s and Fig.6(f) for $t > 3$ s. The desired orbit \mathcal{O}^* is shown in red in both Fig.6(e) and Fig.6(f); it is observed that system trajectories asymptotically converge to \mathcal{O}^* . Finally, $\|e(k)\|_2$, $k = 1, 2, \dots, 40$, is plotted in Fig.6(g), which demonstrates asymptotic convergence of the states $z(k)$ on Σ to z^* .

VI. CONCLUSION

For point-foot planar bipeds, a method for designing and stabilizing impact-free, energy-conserving gaits is presented.

²The expression for u_{hg} uses $\Lambda = I_4$ and $\mu = 0.0005$; the high-gain feedback is terminated when the norm of the error in the active joint velocities reduces below 0.0001.

VHCs are used to design energy-conserving gaits, which are hybrid orbits with a single discontinuity due to coordinate relabelling. A system trajectory that does not lie on such an orbit is subject to discontinuities due to impulsive disturbances arising from foot-ground interaction. To stabilize a desired orbit, we use the ICPM approach, wherein impulsive inputs are applied when the system trajectory intersects a chosen Poincaré section. As the system trajectory converges to the desired orbit, the magnitudes of both the impulsive inputs and impulsive disturbance converge to zero. This approach differs from previous approaches in that impulsive inputs are included in the set of admissible controls. The efficacy of the ICPM approach is demonstrated through a case study of a five-link biped. Future work will focus on search for a wider class of VHCs, and optimal selection of the Poincaré section on which to apply impulsive inputs.

REFERENCES

- [1] J. Grizzle, G. Abba, and F. Plestan, "Asymptotically stable walking for biped robots: analysis via systems with impulse effects," *IEEE Transactions on Automatic Control*, vol. 46, no. 1, pp. 51–64, 2001.
- [2] A. Shiriaev, J. Perram, and C. Canudas-de Wit, "Constructive tool for orbital stabilization of underactuated nonlinear systems: virtual constraints approach," *IEEE Transactions on Automatic Control*, vol. 50, no. 8, pp. 1164–1176, 2005.
- [3] M. Maggiore and L. Consolini, "Virtual Holonomic Constraints for Euler-Lagrange Systems," *IEEE Transactions on Automatic Control*, vol. 58, no. 4, pp. 1001–1008, Apr. 2013.
- [4] E. Westervelt, J. Grizzle, and D. Koditschek, "Hybrid zero dynamics of planar biped walkers," *IEEE Transactions on Automatic Control*, vol. 48, no. 1, pp. 42–56, 2003.
- [5] L. B. Freidovich, A. S. Shiriaev, and I. R. Manchester, "Stability Analysis and Control Design for an Underactuated Walking Robot via Computation of a Transverse Linearization," *IFAC Proceedings Volumes*, vol. 41, no. 2, pp. 10 166–10 171, 2008.
- [6] C. Chevallereau, J. W. Grizzle, and C.-L. Shih, "Asymptotically Stable Walking of a Five-Link Underactuated 3-D Bipedal Robot," *IEEE Transactions on Robotics*, vol. 25, no. 1, pp. 37–50, 2009.
- [7] J. W. Grizzle and C. Chevallereau, "Virtual Constraints and Hybrid Zero Dynamics for Realizing Underactuated Bipedal Locomotion," in *Humanoid Robotics: A Reference*, A. Goswami and P. Vadakkepatt, Eds. Dordrecht: Springer Netherlands, 2019, pp. 1045–1075.
- [8] E. R. Westervelt, F. L. Lewis, J. W. Grizzle, S. S. Ge, C. Chevallereau, J. H. Choi, and B. Morris, *Feedback Control of Dynamic Bipedal Robot Locomotion*. Boca Raton: CRC Press, Oct. 2018.
- [9] M. G. Boroujeni, E. Daneshman, L. Righetti, and M. Khadiv, "A unified framework for walking and running of bipedal robots," in *20th Int. Conference on Advanced Robotics (ICAR)*, 2021, pp. 396–403.
- [10] R. Jafari, L. L. Flynn, A. Hellum, and R. Mukherjee, "Energy-Conserving Gaits for Point-Foot Planar Biped: A Five-DOF Case Study," in *ASME Dynamic Systems and Control Conference*, Palo Alto, CA, 2013.
- [11] N. Kant and R. Mukherjee, "Orbital Stabilization of Underactuated Systems using Virtual Holonomic Constraints and Impulse Controlled Poincaré Maps," *Systems & Control Letters*, vol. 146, p. 104813, 2020.
- [12] —, "Juggling a Devil-Stick: Hybrid Orbit Stabilization Using the Impulse Controlled Poincaré Map," *IEEE Control Systems Letters*, vol. 6, pp. 1304–1309, 2022.
- [13] N. Kant, R. Mukherjee, D. Chowdhury, and H. K. Khalil, "Estimation of the Region of Attraction of Underactuated Systems and Its Enlargement Using Impulsive Inputs," *IEEE Transactions on Robotics*, vol. 35, no. 3, pp. 618–632, 2019.
- [14] Y. Hurmuzlu and D. B. Marghitu, "Rigid Body Collisions of Planar Kinematic Chains With Multiple Contact Points," *The International Journal of Robotics Research*, vol. 13, no. 1, pp. 82–92, 1994.
- [15] C. Byrnes and A. Isidori, "Asymptotic stabilization of minimum phase nonlinear systems," *IEEE Transactions on Automatic Control*, vol. 36, no. 10, pp. 1122–1137, 1991.
- [16] H. Khalil, *Nonlinear Systems*. Prentice Hall, 2002.